Supporting information

Partial Sulfuration-induced Defect and Interface Tailoring on Bismuth Oxide for Promoting Electrocatalytic CO_2 Reduction

Xuxiao Yang,[‡a] Peilin Deng,[‡c] Dongyu Liu,[‡b] Shuang Zhao,[a] Dan Li,[a] Hu Wu,[a] Yaming Ma,[a] Bao Yu Xia,[*c] Mingtao Li,[*b] Chunhui Xiao[*a] and Shujiang Ding[a]

[a]Xi'an Key Laboratory of Sustainable Energy Materials Chemistry, Department of Applied Chemistry, School of Science, Xi'an Jiaotong University, Xianning West Road, Xi'an 710049, China

[b]International Research Center for Renewable Energy, State Key Laboratory of Multiphase Flow in Power Engineering, Xi'an Jiaotong University, Xianning West Road, Xi'an 710049, China

[c]Key Laboratory of Material Chemistry for Energy Conversion and Storage (Ministry of Education), Hubei Key Laboratory of Material Chemistry and Service Failure, School of Chemistry and Chemical Engineering, Wuhan National Laboratory for Optoelectronics, Huazhong University of Science and Technology (HUST), 1037 Luoyu Road, Wuhan, 430074, PR China

‡Xuxiao Yang, Peilin Deng and Dongyu Liu contributed equally to this work.

*Email address for corresponding authors: chunhuixiao@xjtu.edu.cn (C. Xiao), mingtao@mail.xjtu.edu.cn (M. Li), byxia@hust.edu.cn(B. Xia)

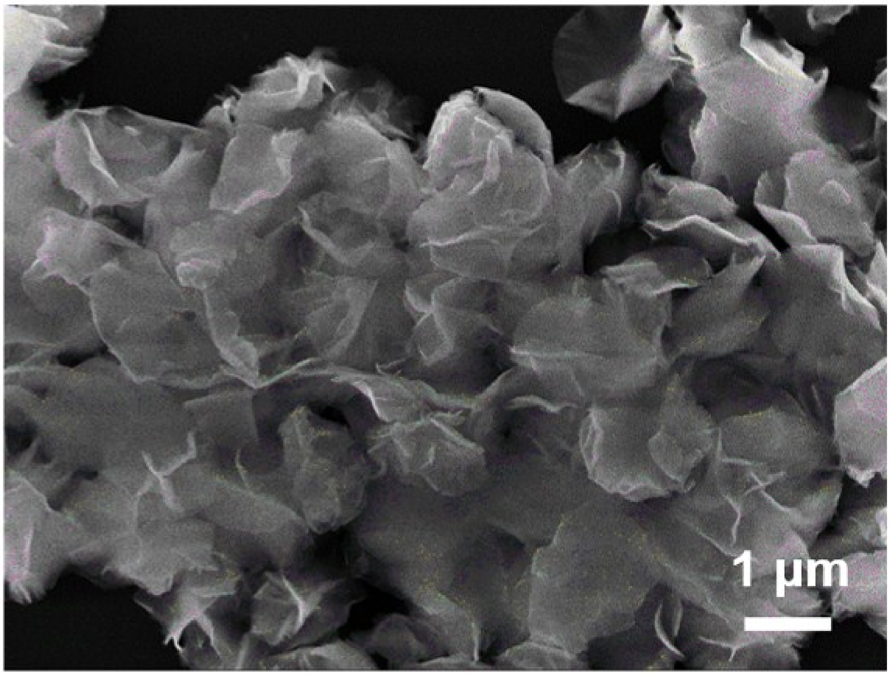

Figure S1. SEM image of Bi_2O_3 nanosheets.

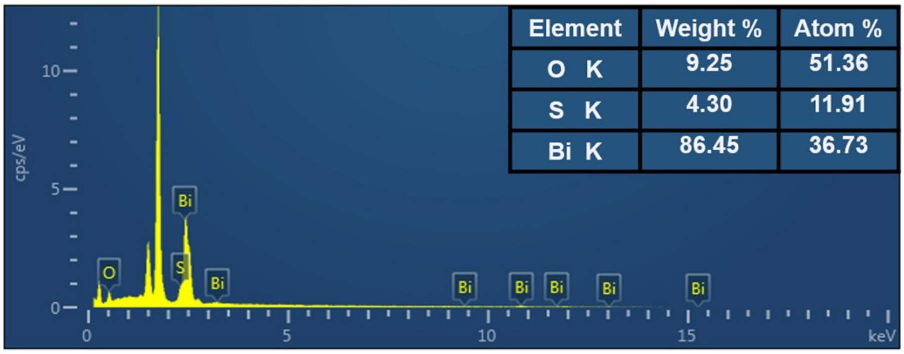

Figure S2. The corresponding energy dispersive X-ray spectroscopy (EDX) of Bi_2S_3-Bi_2O_3 nanosheets.

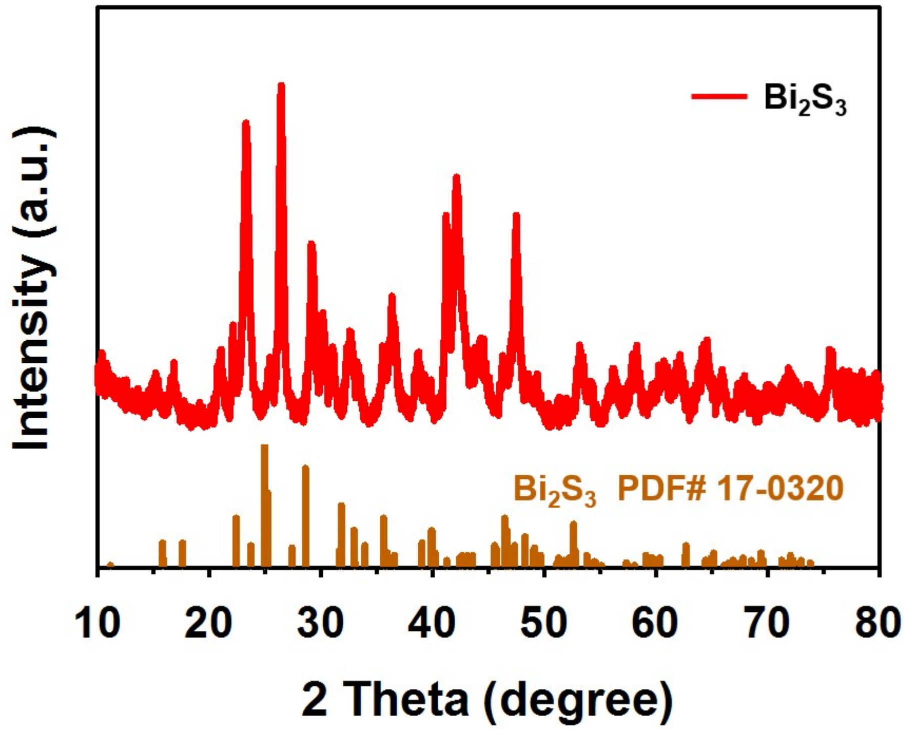

Figure S3. XRD patterns of Bi_2S_3.

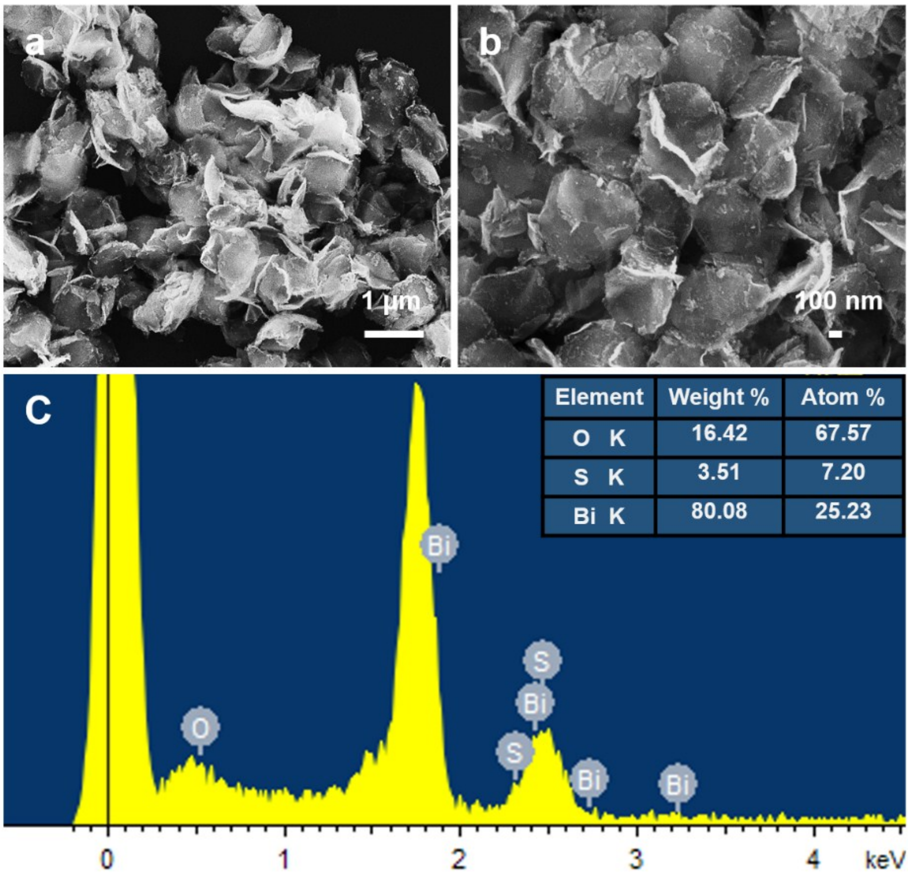

Figure S4. (a, b) SEM images and (c) the corresponding energy dispersive X-ray spectroscopy (EDX) of Bi_2S_3-Bi_2O_3-0.5.

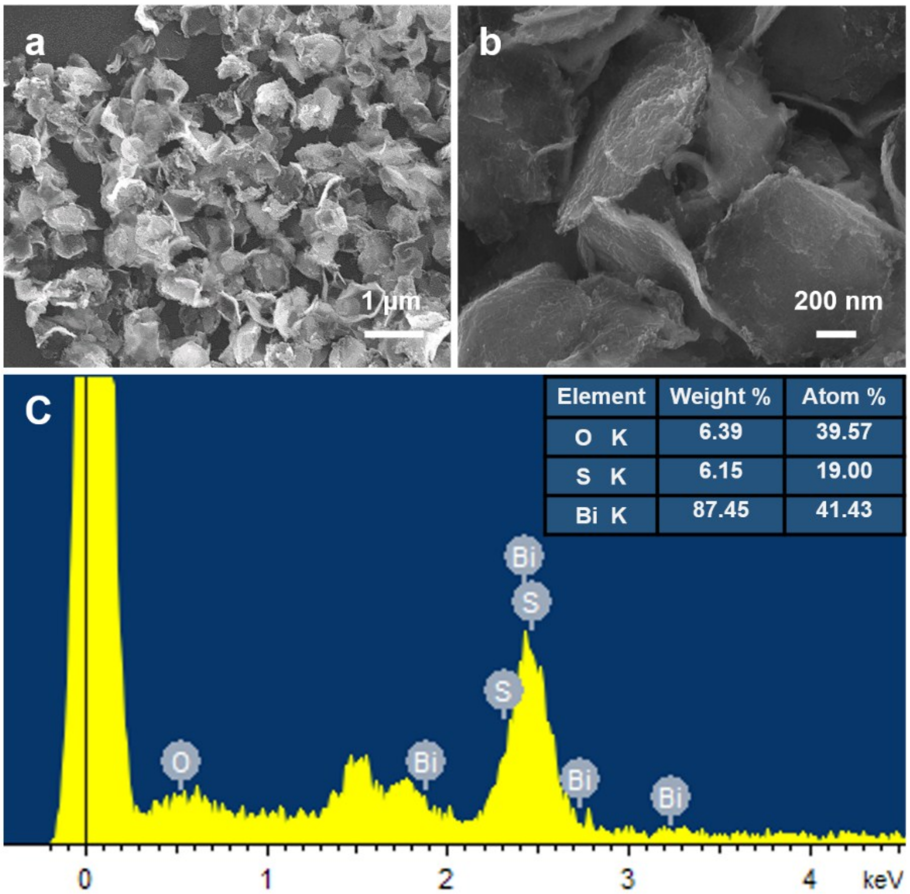

Figure S5. (a, b) SEM images and (c) the corresponding energy dispersive X-ray spectroscopy (EDX) of Bi_2S_3-Bi_2O_3-2.

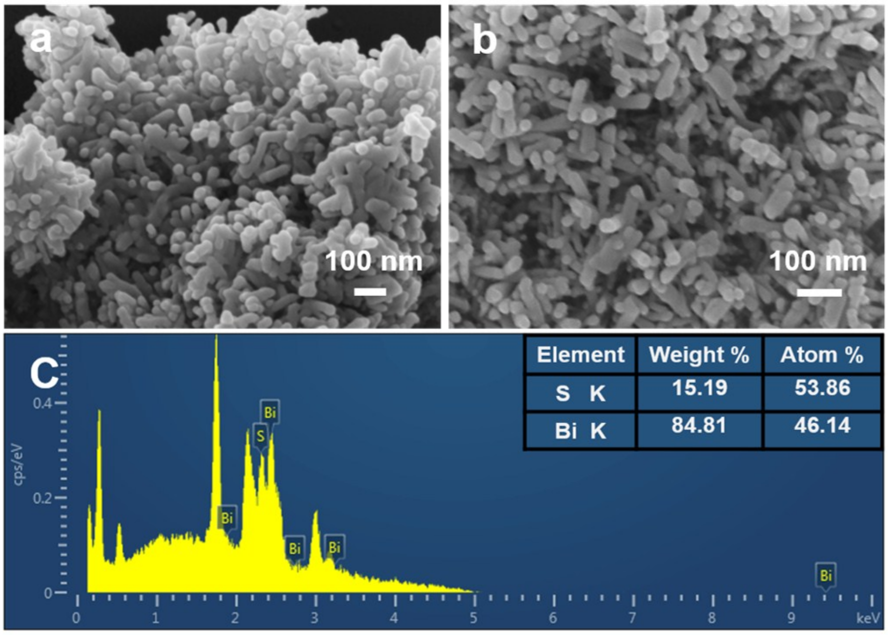

Figure S6. (a, b) SEM images and (c) the corresponding energy dispersive X-ray spectroscopy (EDX) of Bi_2S_3.

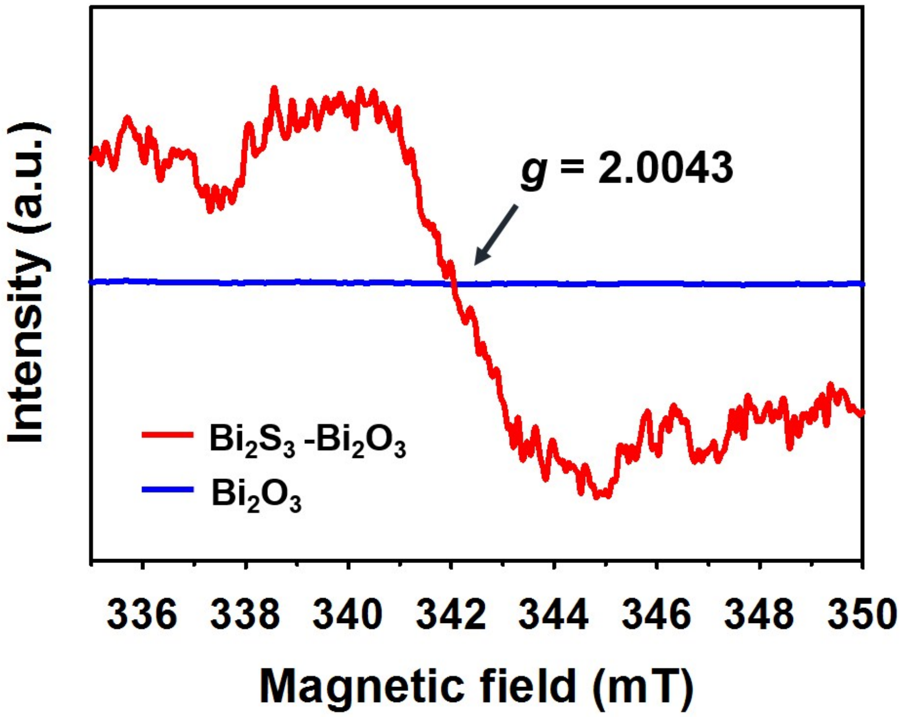

Figure S7. EPR spectra of Bi_2S_3 -Bi_2O_3 (red) and Bi_2O_3 (blue) at room temperature.

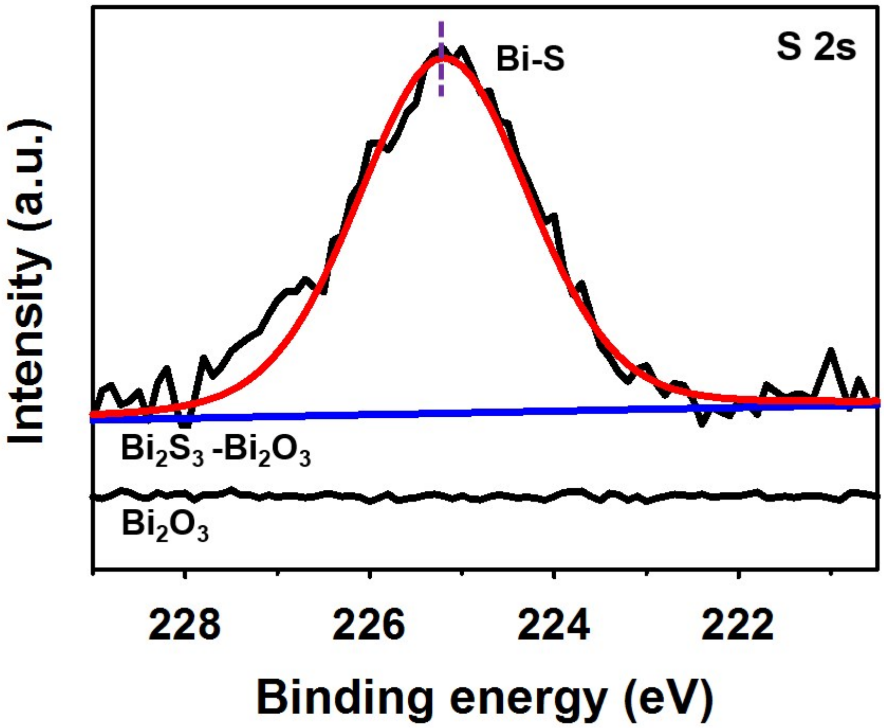

Figure S8. High-resolution XPS spectra of S 2s in Bi_2S_3-Bi_2O_3 and Bi_2O_3.

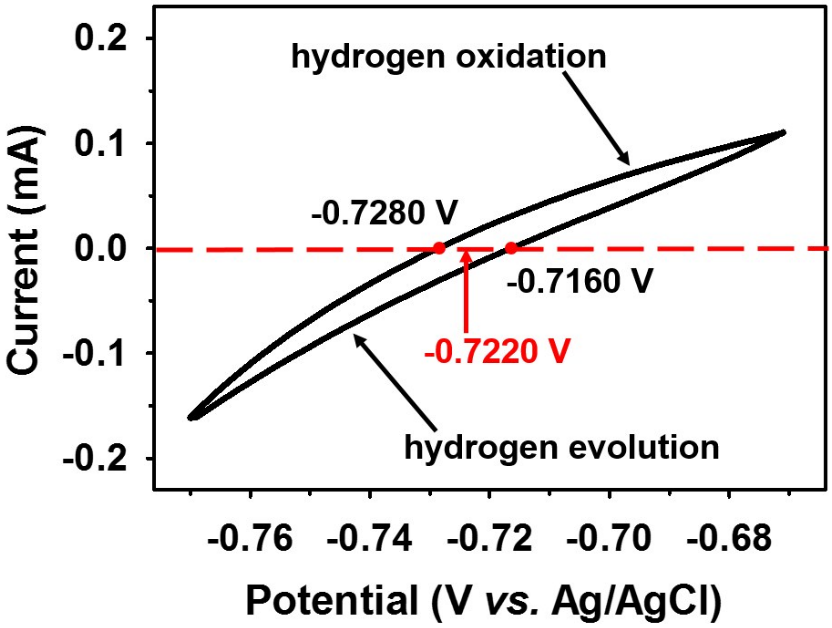

Figure S9. The RHE calibration was measured in the high purity H_2-saturated electrolyte (0.1 M $KHCO_3$). Pt foils act as both the working electrode and counter electrode through cyclic voltammetry (CV) at a scan rate of 1 mV s^{-1}, and the average of two potentials at which the current crossed zero was taken to be the thermodynamic potential for the hydrogen electrode reactions[1]. So in 0.1 M $KHCO_3$, $E_{(RHE)} = E_{(Ag/AgCl)} + 0.722V$

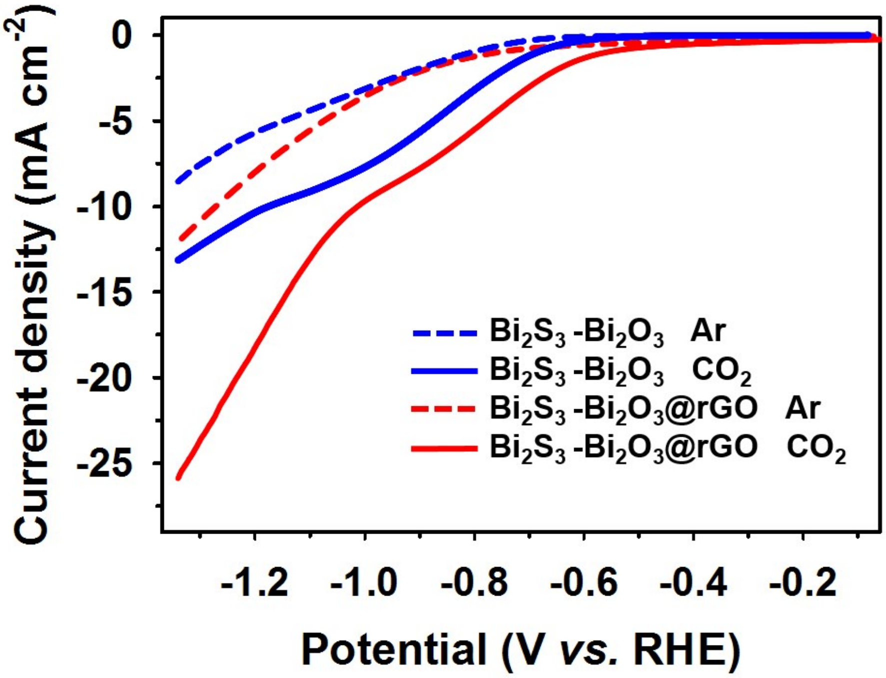

Figure S10. Linear sweep voltammetry (LSV) curves of Bi_2S_3-Bi_2O_3@rGO (red) and Bi_2S_3-Bi_2O_3 (blue) at a scan rate of 5 mV s^{-1} in Ar and CO_2-saturated 0.1 M $KHCO_3$ solution.

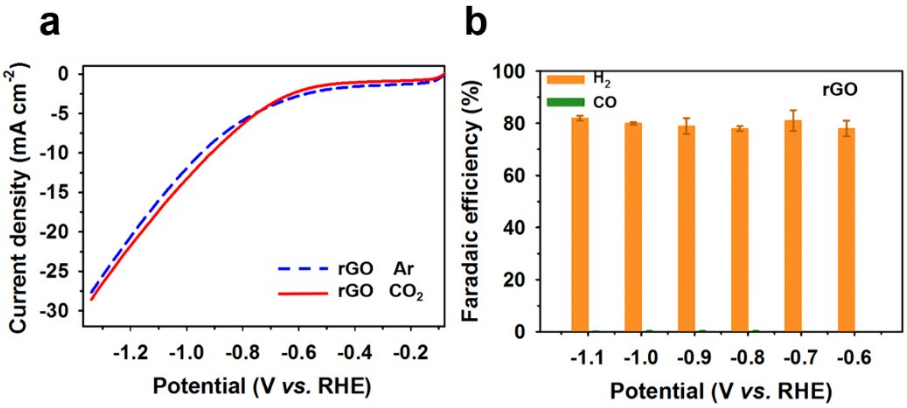

Figure S11. (a) Linear sweep voltammetry (LSV) curves of rGO at a scan rate of 5 mV s^{-1} in Ar and CO_2 saturated 0.1 M $KHCO_3$ solution. (b) Faradaic effciency of rGO for CO_2 reduction at each applied potential for 2 h.

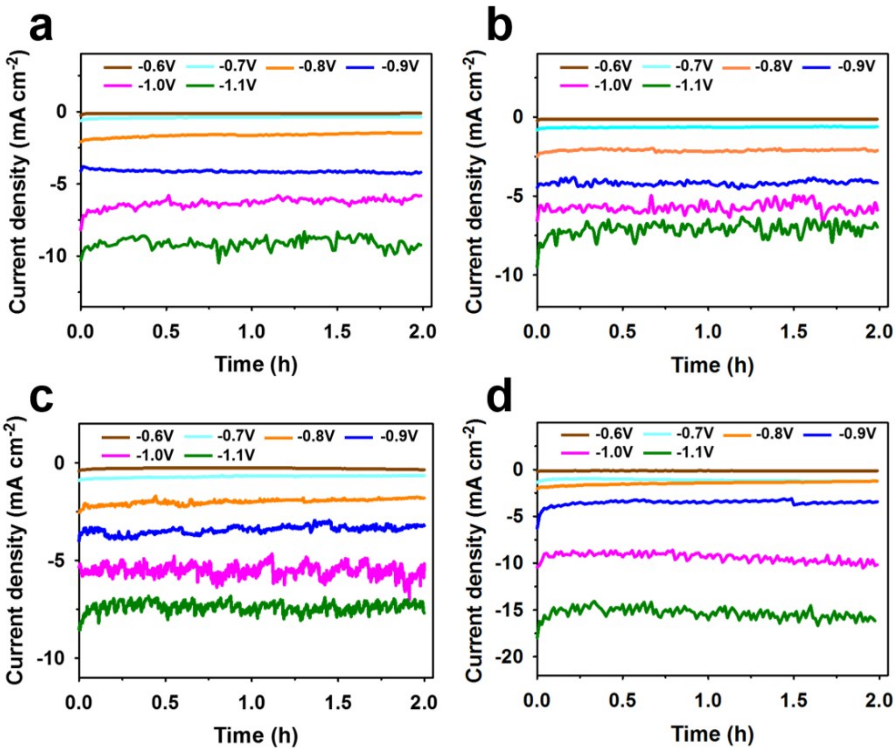

Figure S12. Chronopotentiometric curves at the corresponding potentials in CO_2-saturated 0.1 M $KHCO_3$ solution on (a) Bi_2S_3-Bi_2O_3@rGO (b) Bi_2O_3@rGO, (c) Bi_2S_3@rGO and (d) rGO, respectively.

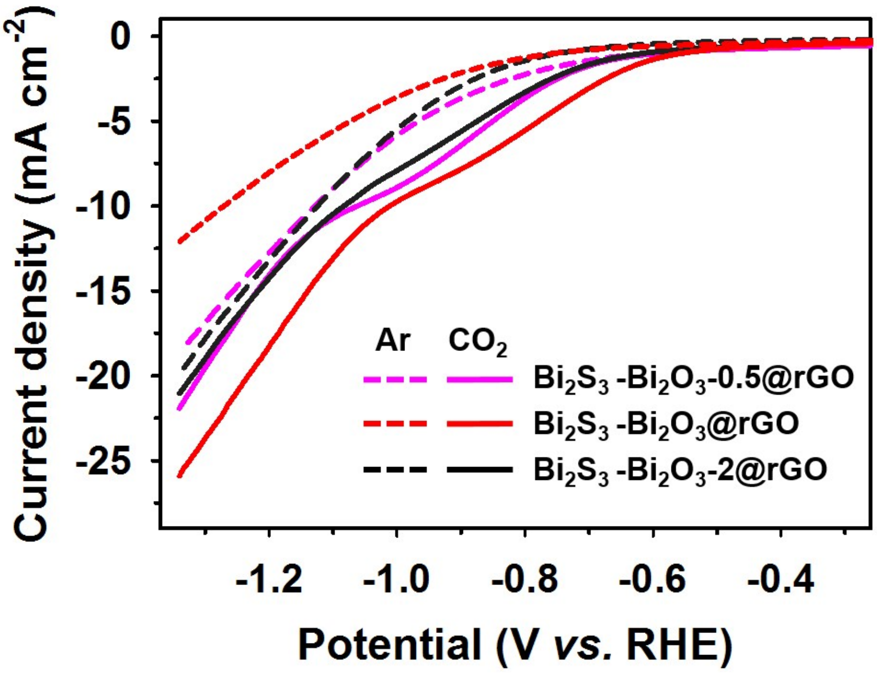

Figure S13. Linear sweep voltammetry (LSV) curves of Bi_2S_3-Bi_2O_3-0.5@rGO (peach pink), Bi_2S_3-Bi_2O_3@rGO (red) and Bi_2S_3-Bi_2O_3-2@rGO (black) at a scan rate of 5 mV s^{-1} in Ar and CO_2-saturated 0.1 M $KHCO_3$ solution.

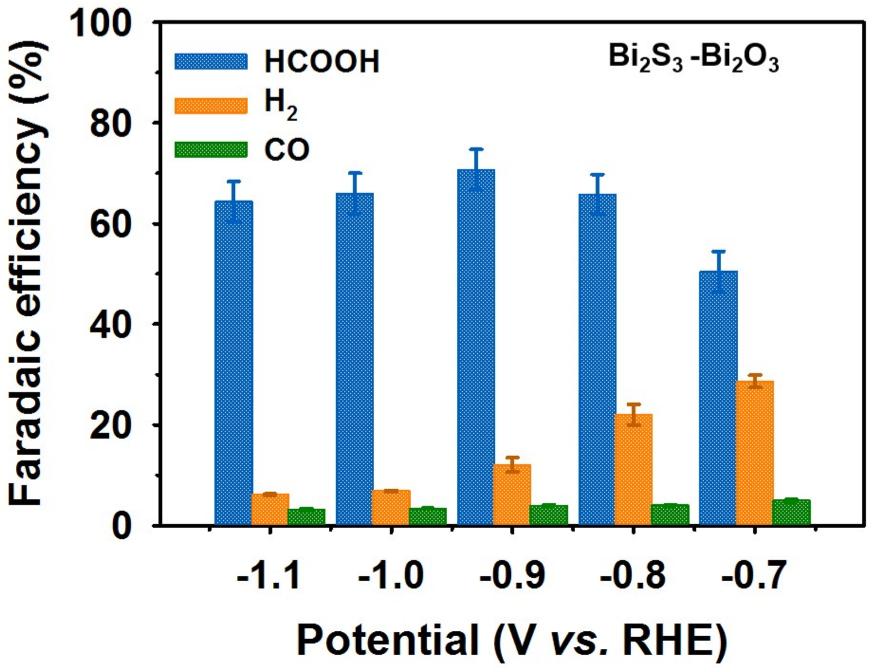

Figure S14. Faradaic efficiency of Bi_2S_3-Bi_2O_3 for CO_2 reduction at each applied potential for 2 h.

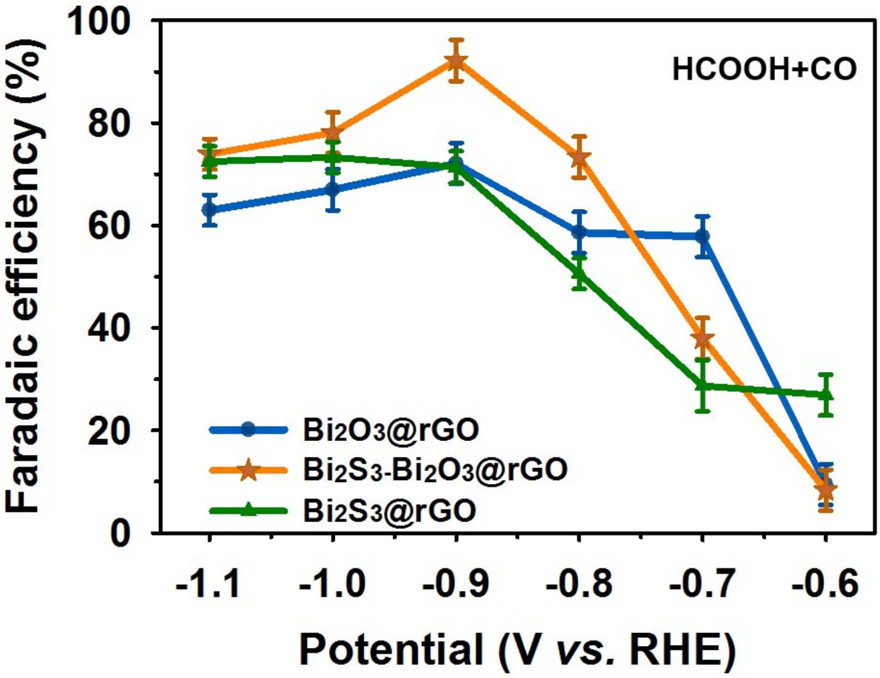

Figure S15. Faradaic efficiencies for HCOOH and CO on Bi_2S_3-Bi_2O_3@rGO (orange), Bi_2O_3@rGO (blue) and Bi_2S_3@rGO (green) at different applied potentials.

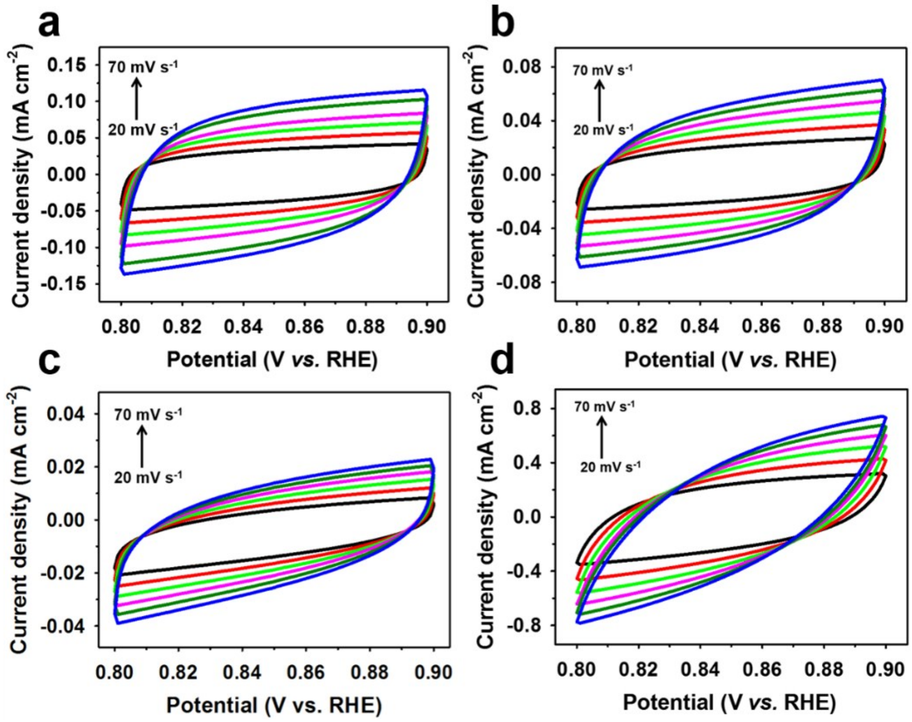

Figure S16. Double layer capacitance (Cdl) obtained from cyclic voltammograms of (a) Bi_2S_3-Bi_2O_3@rGO (b) Bi_2O_3@rGO, (c) Bi_2S_3@rGO and (d) rGO in CO_2-saturated 0.1 M $KHCO_3$ electrolyte between 0.80 V and 0.90 V vs. RHE at various scan rates, respectively.

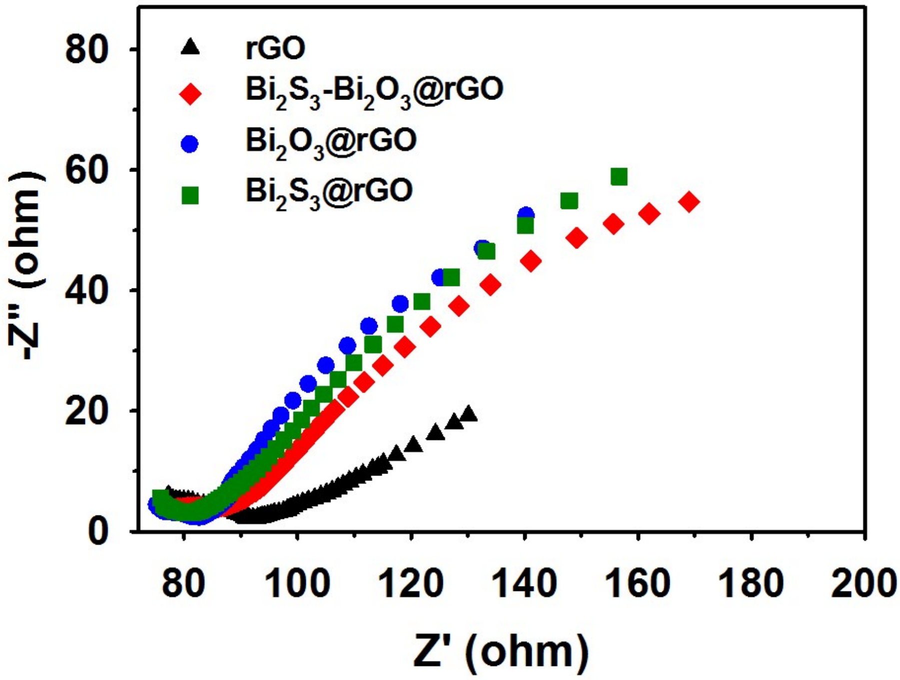

Figure S17. Electrochemical impedance spectroscopy (EIS) curves of Bi_2S_3-Bi_2O_3@rGO, Bi_2O_3@rGO, Bi_2S_3@rGO and rGO catalysts performed in CO_2 -saturated 0.1 M $KHCO_3$ solution at -0.9 V vs. RHE.

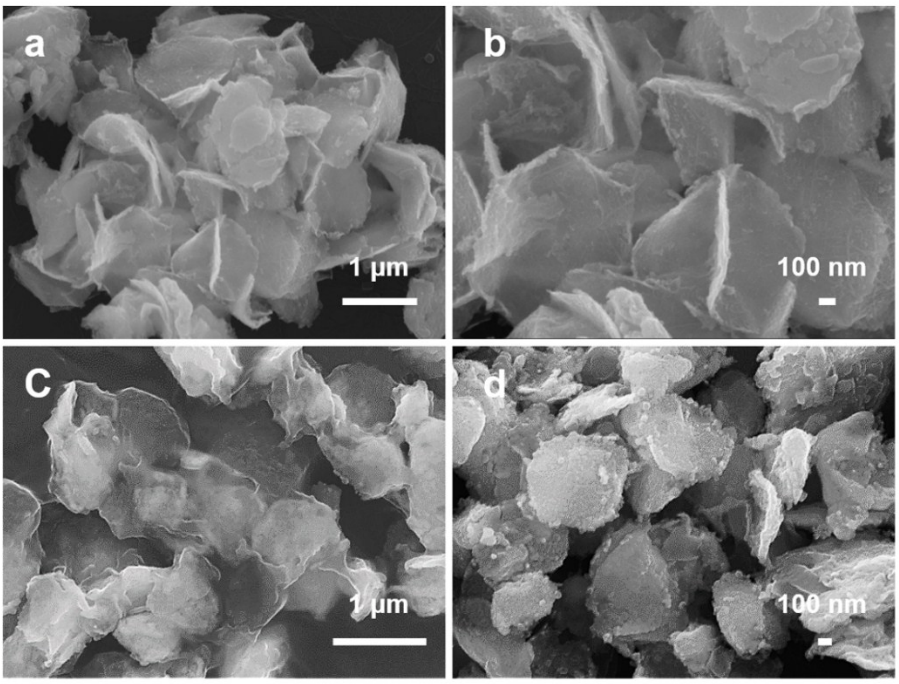

Figure S18. SEM images of Bi_2S_3-Bi_2O_3@rGO (a, b) before and (c, d) after 24 h electrolysis.

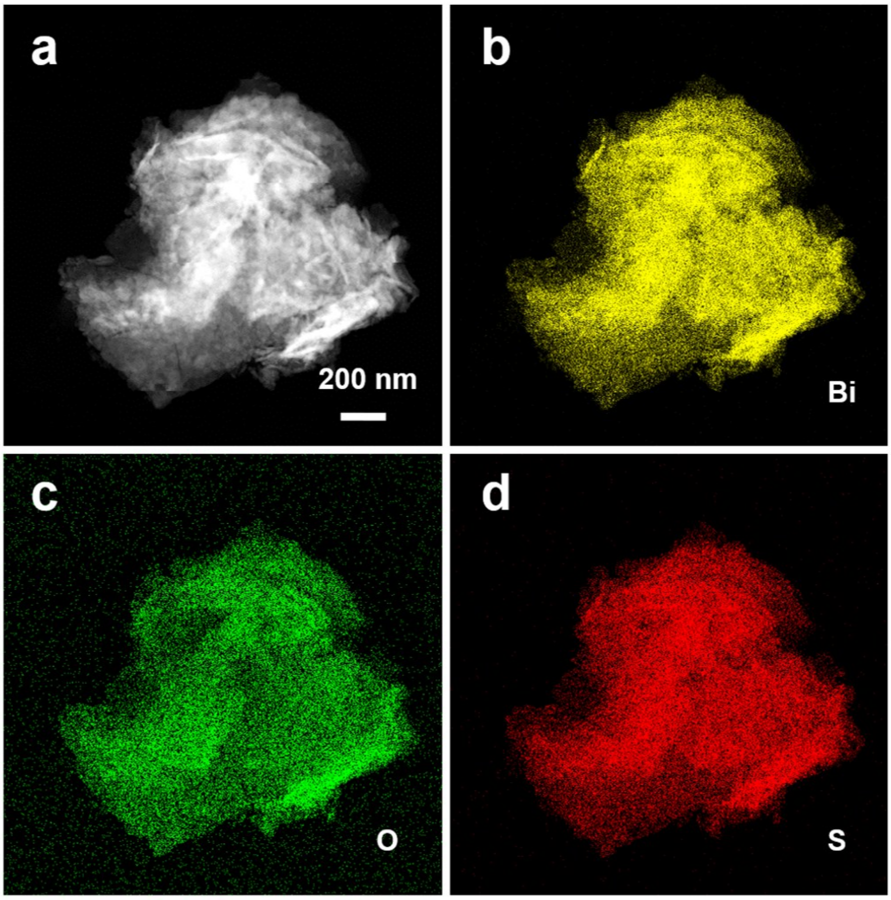

Figure S19. TEM mapping of Bi_2S_3-Bi_2O_3@rGO after 24 h electrolysis.

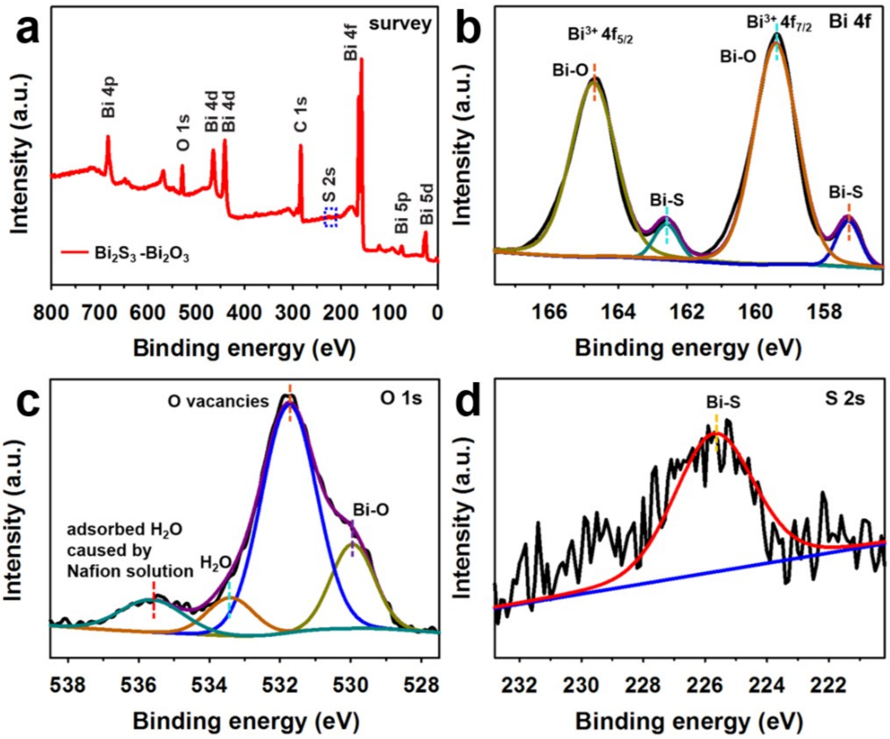

Figure S20. XPS spectra of Bi_2S_3-Bi_2O_3@rGO (a) survey scan, (b) Bi 4f, (c) O 1s, and (d) S 2s after 24 h electrolysis.

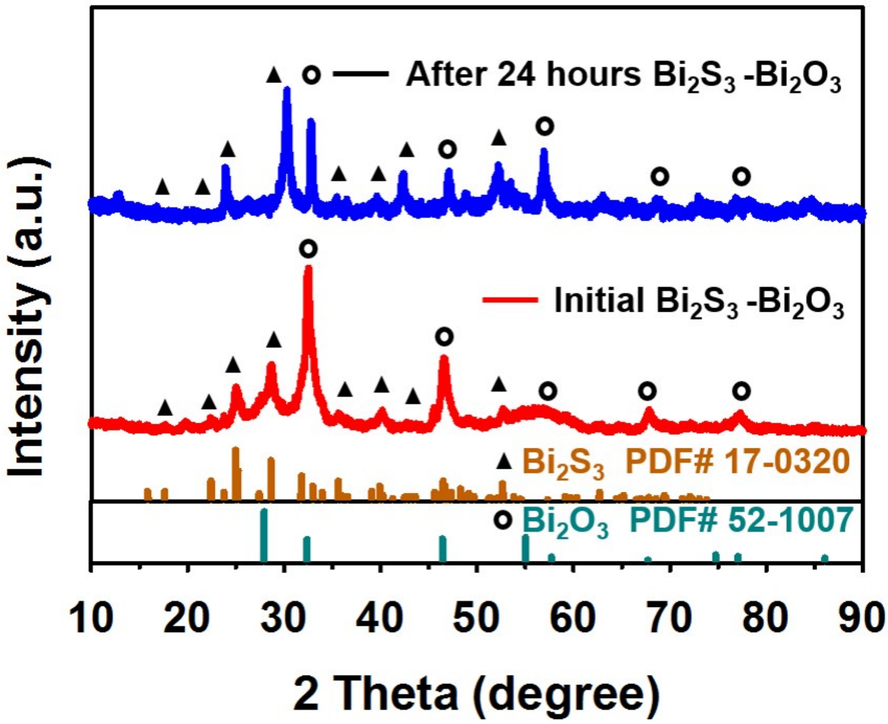

Figure S21. XRD patterns of Bi_2S_3-Bi_2O_3@rGO before and after 24 h electrolysis.

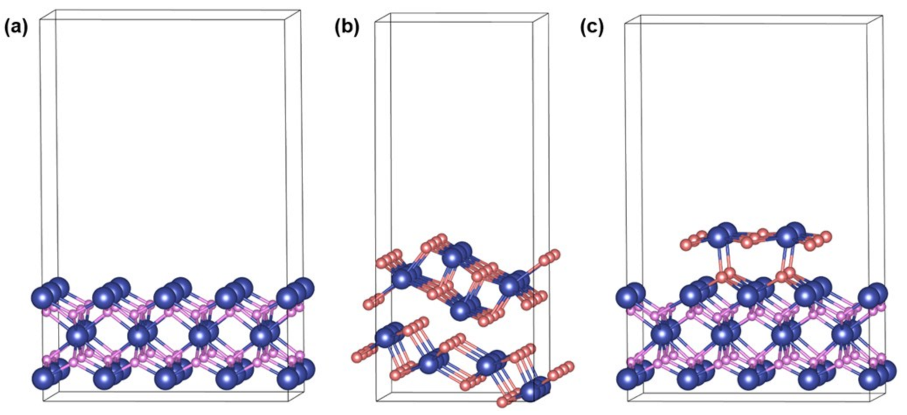

Figure S22. The structures of (a) Bi_2O_3 (200) surface, (b) Bi_2S_3 (100) surface and (c) Bi_2S_3-Bi_2O_3 heterostructure. The Bi, O, S atoms are denoted by blue, pink and red balls, respectively.

Table S1. Calculated total energies of different surface models with different k-points mesh.

	1×3×1	**2×3×1**	**2×4×1**
Bi_2O_3 (200)	-312.07 eV	-312.36 eV	-312.34 eV
Bi_2O_3-Bi_2S_3	-381.55 eV	-381.47 eV	-381.43 eV
	1×1×1	2×2×1	3×3×1
Bi_2S_3 (100)	-270.68 eV	-271.01 eV	-271.01 eV

Table S2. Comparison of the electrocatalytic performance for reducing CO_2 to formate on different Bi-based electrodes reported recently.

Electrocatalysts	**Electrolyte**	**Potential (*vs.* RHE)**	**FE_{HCOOH}**	**Durability**	**Ref.**
Bi_2S_3-Bi_2O_3@rGO	0.1M $KHCO_3$	-0.9V	90.1%	24h	This work
Bi nanosheets	0.5M $NaHCO_3$	-0.9V - -1.2V	90%	5 h	[2]
Bi	0.5 M $KHCO_3$	-0.82 V	82%	6h	[3]
Bi subcarbonate	0.5M Na_2CO_3	-0.7 V	85%	12h	[4]
Bi dendrite catalyst	0.5 M $KHCO_3$	−0.74V	89%	12 h	[5]
Bi nanosheets	0.5M $NaHCO_3$	-1.74V vs. SCE	90%	10 h	[6]
Bi_2O_3 nanoparticles	0.5M $NaHCO_3$	-1.2V	91%	23 h	[7]

References

1. C. Xiao, B. Zhang and D. Li, *Electrochim. Acta*, 2017, **242**, 260-267.
2. P. Su, W. Xu, Y. Qiu, T. Zhang, X. Li and H. Zhang, *ChemSusChem*, 2018, **11**, 848-853.
3. E. Bertin, S. Garbarino, C. Roy, S. Kazemi and D. Guay, *J.CO2 Util.*, 2017, **19**, 276-283.
4. Y. Zhang, X. Zhang, Y. Ling, F. Li, A. M. Bond and J. Zhang, *Angew. Chem.*, 2018, **130**, 13467-13471.
5. J. H. Koh, D. H. Won, T. Eom, N.-K. Kim, K. D. Jung, H. Kim, Y. J. Hwang and B. K. Min, *ACS Catal.*, 2017, **7**, 5071-5077.
6. N. Han, Y. Wang, H. Yang, J. Deng, J. Wu, Y. Li and Y. Li, *Nat. Commun.*, 2018, **9**, 1320.
7. C.-C. Miao and G.-Q. Yuan, *ChemElectroChem*, 2018, **5**, 3741-3747.